Available online at www.sciencedirect.com
SCIENCE DIRECT®
C. R. Physique 6 (2005) 876–887
COMPTES RENDUS PHYSIQUE
http://france.elsevier.com/direct/COMREN/

Spectroscopy and planetary atmospheres/Spectroscopie et atmosphères planétaires

Spectroscopic challenges for high accuracy retrievals of atmospheric CO_2 and the Orbiting Carbon Observatory (OCO) experiment

Charles E. Miller [a,*], Linda R. Brown [a], Robert A. Toth [a], D. Chris Benner [b], V. Malathy Devi [b]

[a] *Jet Propulsion Laboratory, California Institute of Technology, Pasadena, CA 91109-8099, USA*
[b] *Department of Physics, College of William and Mary, Williamsburg, VA 23187-8795, USA*

Abstract

The space-based Orbiting Carbon Observatory (OCO) mission will achieve global measurements needed to distinguish spatial and temporal gradients in the CO_2 column. Scheduled by NASA to launch in 2008, the instrument will obtain averaged dry air mole fraction (X_{CO_2}) with a precision of 1 part per million (0.3%) in order to quantify the variation of CO_2 sources and sinks and to improve future climate forecasts. Retrievals of X_{CO_2} from ground-based measurements require even higher precisions to validate the satellite data and link them accurately and without bias to the World Meteorological Organization (WMO) standard for atmospheric CO_2 observations. These retrievals will require CO_2 spectroscopic parameters with unprecedented accuracy. Here we present the experimental and data analysis methods implemented in laboratory studies in order to achieve this challenging goal. ***To cite this article: C.E. Miller et al., C. R. Physique 6 (2005).***

Résumé

Défis spectroscopiques pour la détermination ultra-précise des quantités de CO_2 atmosphérique par l'expérience Orbiting Carbon Observatory (OCO). La mission spatiale *Orbiting Carbon Observatory* (*OCO*) fournira les mesures globales nécessaires pour étudier les gradients spatiaux et temporels des quantités de CO_2 dans notre atmosphère. Avec une mise en orbite prévue par la NASA en 2008, cet instrument déterminera la fraction molaire (X_{CO_2}) moyenne avec une précision de une partie par million (1 ppm, 0.3%) afin de quantifier les variations des sources et puits de CO_2 et d'améliorer les prévisions météorologiques à venir. Les déterminations de X_{CO_2} à partir du sol devront avoir une précision encore supérieure afin de valider les données satellites pour qu'elles satisfassent, sans biais, les standards de la *World Meteorological Organization* (*WMO*) pour ce qui concerne les observations du CO_2 atmosphérique. Ces mesures par télédétection dans l'infrarouge proche nécessiteront de connaître les paramètres spectroscopiques avec une précision sans précédent. Cet article présente les méthodes expérimentales et d'analyse des données qui sont développées au laboratoire afin d'atteindre cet objectif. ***Pour citer cet article : C.E. Miller et al., C. R. Physique 6 (2005).***

* Corresponding author. Charles E. Miller, Jet Propulsion Laboratory, MS 183-501, 4800 Oak Grove Drive, Pasadena, CA 91109-8099, USA. Tel.: +1 818 393 6294; fax: +1 818 354 0966.
E-mail address: charles.e.miller@jpl.nasa.gov (C.E. Miller).

1631-0705/$ – see front matter
doi:10.1016/j.crhy.2005.09.005

Keywords: Carbon dioxide (CO_2); Orbiting Carbon Observatory (OCO); Near infrared spectroscopy

Mots-clés : Dioxyde de carbone (CO_2) ; Orbiting Carbon Observatory (OCO) ; Spectroscopie proche infrarouge

1. Introduction

Carbon dioxide (CO_2) is a natural component of the Earth's atmosphere and for more than a century it has been known to be a strong greenhouse forcing agent. In the late 1950s Keeling established a record of regular, extremely accurate surface in situ measurements demonstrating that global CO_2 levels have been increasing persistently [1]. These data, combined with data from the recent geologic record, show that human activity in the form of fossil fuel combustion, change in land use, etc. has driven atmospheric CO_2 concentrations from 280 ppm to greater than 370 ppm since the dawn of the industrial era [2,3]. However, only about half of the CO_2 emitted from fossil fuel combustion over the last 40 years has accumulated in the atmosphere. The remainder has been absorbed by the oceans and the terrestrial biosphere (examples of CO_2 sinks). The accumulation of atmospheric CO_2 could accelerate if the efficiencies of these CO_2 sinks decrease in the future [4,5], but our current understanding of the nature, geographic distribution and temporal variability of CO_2 sinks is inadequate to predict their responses to future climate or land use changes. Observational system simulation experiments indicate that uncertainties in the atmospheric CO_2 budget could be significantly reduced if data from the current network of surface in situ CO_2 measurements were combined with spatially resolved, global, retrievals of the CO_2 column-integrated dry air mole fraction (X_{CO_2}) having precisions of 1–2 ppm (0.3–0.5% of 370 ppm) [6]. The Orbiting Carbon Observatory (OCO) has been designed to provide space-based X_{CO_2} data with the precision, resolution, and coverage needed to characterize CO_2 sources and sinks on regional scales.

The OCO mission concept and a derivation of the measurement precision requirements for space-based X_{CO_2} data have been presented elsewhere [7,8]. Here we summarize the salient details. The Observatory (Fig. 1) will carry a single instrument that incorporates three bore-sighted high-resolution spectrometers designed to measure reflected sunlight in the 0.76-μm O_2 A-band and in the 1.61 and 2.06 μm CO_2 bands. High-resolution spectroscopic observations of near infrared CO_2 absorption bands in reflected sunlight are selected for this application because they provide high sensitivity near the surface, where most CO_2 sources and sinks are located. Measurements from thermal infrared sounders such as TOVS and AIRS may also be used to retrieve atmospheric CO_2 [9–12], but these data lack crucial information about CO_2 sinks since they are most sensitive to CO_2 concentrations in the middle and upper troposphere and have little sensitivity near the surface. To minimize systematic errors, X_{CO_2} will be retrieved from the CO_2/O_2 ratio derived from simultaneous collocated soundings. The OCO mission includes rigorous on-orbit calibration procedures and a comprehensive validation program to ensure that the radiances and space-based X_{CO_2} data have precisions of 0.3% on regional scales. These efforts will standardize the OCO X_{CO_2} retrievals to the WMO scale for atmospheric CO_2 measurements to facilitate data assimilation and synthesis inversion modeling efforts to quantify CO_2 sources and sinks.

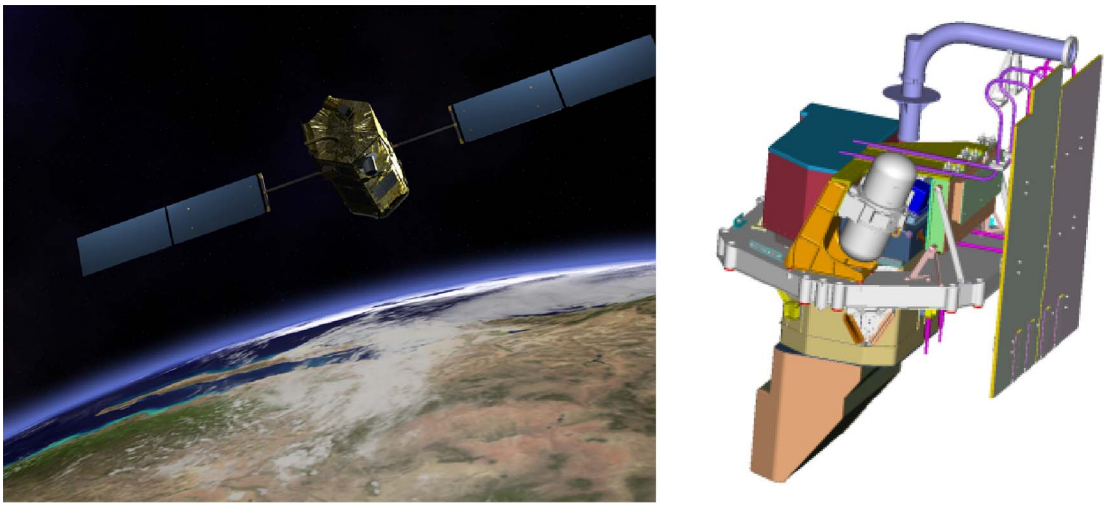

Fig. 1. Left: Artist's conception of the Orbiting Carbon Observatory operating in NADIR pointing mode. Right: Mechanical drawing of the OCO instrument.

OCO X_{CO_2} precision requirements place unprecedented demands on the CO_2 spectroscopic parameters that are needed as inputs for atmospheric radiative transfer (forward) models to retrieve X_{CO_2} from measured radiances. The design of OCO instrumentation, observational strategies, calibration and validation, as well as the interpretation of the current archive of atmospheric spectra all require extensive knowledge of the line-by-line parameters associated with the observed spectral features in the 4000–10 000 cm^{-1} range. Typically, hundreds to thousands of individual rotation–vibration transitions contribute to the signature of a particular CO_2 spectral window. The line-by-line parameters must be in electronic form so that they can be easily manipulated in radiative transfer computations. The spectroscopic parameters needed are line center frequencies or line positions ν, the lower state transition energies E'', the transition line intensities I, and the temperature dependent line shape parameters. The line shapes are characterized by the Doppler widths $\Delta\nu_D$, the Lorentz widths γ and pressure shifts δ associated with collisional broadening by foreign gas species, and, for gases such as CO_2, by line mixing.

In the past, spectroscopic remote sensing experiments have used CO_2 transitions extensively to retrieve temperature and pressure profiles or determine pointing location based on the assumption that CO_2 is uniformly mixed throughout the atmosphere [13,14]. However, the OCO objective is to measure directly small spatial and temporal variations in X_{CO_2}. The general sensitivities of the line parameters for abundance determination are well established: at pressures near one atmosphere, errors in the intensity and half widths are known to propagate linearly, but the influence of the pressure-induced shifts in line positions is often ignored. For example, Devi et al. [15,16] showed that the inclusion of the proper pressure shift parameter reduces the standard deviation of the atmospheric retrieval for a CO_2 line in the 10 μm laser bands by a factor of 10. The impact of pressure shifts on OCO retrievals will be magnified since the magnitude of the shifts is roughly proportional to the transition frequency. Despite these known requirements, the HITRAN 2004 database [23] contains CO_2 pressure shifts for only the ν_3 fundamental at 4.3 μm and the $\nu_3 - \nu_1$ and $\nu_3 - 2\nu_2$ 'laser bands' at 10 μm.

Ground-based high-resolution solar spectra recorded in the near infrared provide opportunities to generate high quality X_{CO_2} retrievals and validate the accuracy of the CO_2 spectroscopic parameters. Wallace and Livingston first demonstrated the ability to use ground-based high-resolution NIR spectra for remote sensing of column CO_2 by using solar spectra recorded with the McMath–Pierce FTS at the Kitt Peak National Solar Observatory over a period from 1979–1985 [17]. They showed that precise measurements of total column CO_2 could be obtained by ratioing CO_2 abundances determined from the $30012 \leftarrow 00001$ band ($\nu_0 = 6348$ cm^{-1}) by the total column O_2 abundance determined from spectroscopic detection of the $^1\Delta_g \leftarrow {}^3\Sigma_u^-$ transition ($\nu_0 = 7882$ cm^{-1}). Wallace and Livingston noted the failure of simple Voigt line shape functions to describe the observed spectra correctly [17]. Yang et al. reanalyzed the Kitt Peak solar spectra using a more sophisticated retrieval algorithm and updated spectroscopic parameters [18]. They demonstrated an impressive 0.5% measurement precision in retrieved values of X_{CO_2} with the remaining errors dominated by deficiencies in the spectroscopic parameters. This led them to conclude that solar viewing Fourier transform spectrometry will be adequate for validating space-based CO_2 column observations [18].

In previous remote sensing applications it was possible to neglect characterization of weakly absorbing transitions since only the strong CO_2 transitions were used for retrievals [6,17,19]. However, knowledge of the spectroscopic parameters for the strong CO_2 transitions alone is insufficient to meet the 0.3% X_{CO_2} precision goals since the weaker transitions will overlap with and contribute to the line shapes of the strong transitions [17,20–22]. Furthermore, the weaker transitions will have different temperature dependences, pressure broadening, and pressure shift characteristics than the stronger transitions, requiring the best possible knowledge of the line-by-line parameters for all CO_2 transitions in the near infrared spectral window above the 0.3% threshold to ensure precise remote sensing retrievals.

Table 1 summarizes the current state of knowledge for CO_2 line-by-line parameters and the accuracies required for OCO and other carbon cycle remote sensing applications. Comparing the entries demonstrates that the HITRAN spectral parameters [23] do not support the stringent 0.3% precision requirements, despite efforts already underway to monitor atmospheric CO_2 from the ground [17,18] and from space [6,19] using near infrared detection. The need for more sensitive remote sensing measurements and the increasing sophistication in remote sensing instrumentation drives the demand for better line-by-line

Table 1
Remote sensing requirements for atmospheric CO_2

Parameter	Mid-IR remote sensing precision requirement	OCO remote sensing precision requirement
Column CO_2 uncertainty	Best effort	<0.3%
Range	600–2500 cm^{-1}	4000–6500 cm^{-1}
Line position uncertainty	0.0003 cm^{-1}	<0.0002 cm^{-1}
E'' uncertainty	0.5%	<0.1%
Line intensity uncertainty	<3%	0.3%
Lorentz width uncertainty	<3%	0.6%
Pressure shift uncertainty	<0.0003 cm^{-1} atm^{-1}	<0.0002 cm^{-1} atm^{-1}
Line mixing	Q-branches only	P-, Q- and R-branches

reference parameters. These remote sensing requirements pose several fundamental challenges to laboratory spectroscopists: Can absolute (or even relative) intensities and line shape parameters be measured to the required 0.3% accuracy for a polyatomic molecule? Are there new, unanticipated aspects of the typical line position/line intensity/line shape problem that are revealed at this level of scrutiny? Will these investigations reveal new physics or demonstrate a new paradigm for the spectroscopic parameters needed to reproduce atmospheric remote sensing data quantitatively? The compelling science questions surrounding the global carbon cycle and the status of CO_2 as the textbook example for polyatomic spectroscopy make this an ideal test case for defining how well one can improve the accuracy of the laboratory measurements.

2. Strategies for new laboratory studies

Birk and coworkers have shown that rigorous characterization of the experimental state is critical to obtain the most accurate spectral line parameters possible and that the system/apparatus can be characterized to exacting standards [24]. One must focus on the physical aspects of the measurements that might alter the ability to measure accurately for example, the spectral line positions and intensities, pressure broadening and pressure shift. For OCO, improving the accuracy of the CO_2 line parameters requires that an upgraded multispectrum retrieval technique be applied to high quality spectra recorded with superior knowledge and control of the experimental state as well as improvements to the experimental procedure. Most importantly, spectra must be recorded using an excellent spectrometer with well characterized instrumental line shape and also configured with detectors of minimal non-linearity. High signal to noise ratios (2000 : 1) at Doppler-limited resolution and long-term instrument stability are required.

2.1. Spectral resolution

To deliver CO_2 spectroscopic parameters that satisfy the OCO precision requirements, several laboratory spectra must be recorded with the spectral resolution that achieves the optimal balance of spectral precision and S/N performance for each spectrum. Doppler halfwidths of CO_2 transitions in the 4795–4895 cm^{-1} spectral window vary from 0.004984 cm^{-1} at 370 K to 0.003664 cm^{-1} at 200 K; Doppler widths for transitions in the 6140–6400 cm^{-1} spectral window vary from 0.00651 cm^{-1} at 370 K to 0.004787 cm^{-1} at 200 K. The 0.0114 cm^{-1} resolution used to acquire the spectra in previous work [25,26] (Fig. 2), provided excellent S/N and sampled at least two points for each Doppler limited line shape, satisfying the Nyquist requirement. Oversampling of the line shapes is possible for pressure broadened spectra since the widths are larger than the Doppler limit. Pressure broadened spectra are important for the accurate determination of the phase error, Lorentz widths, Dicke narrowing, and the effects of line mixing since for a given experimental resolution these spectra sample the line shape contour with more points per full width. Line mixing in particular can be determined most accurately from spectra recorded with the highest pressure broadening since pressure increases the effective overlap of the far wings of adjacent transitions.

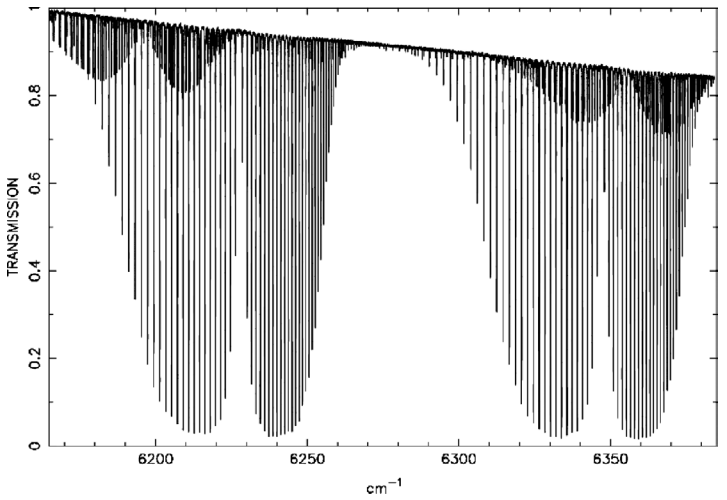

Fig. 2. Detail of the 30013 ← 00001 and 30012 ← 00001 bands from a CO_2 spectrum recorded with the McMath–Pierce FTS. Resolution: 0.011 cm^{-1}; Pressure = 80 Torr; Path = 49 m.

2.2. Temperature and pressure monitoring

We are giving special consideration of how the gas temperatures should be measured. In the past, we have often placed one or two sensors (depending upon the cell length) on the exterior surface of the absorption cell and recorded the average of the temperatures from the beginning and end of each scan. Differences of 2 K were considered acceptable because the molecular number density would change at most by 1%, and the goal was to obtain intensity accuracies of about 2 to 3%. To meet the OCO challenge of measuring intensities to 0.3% accuracy, temperature induced uncertainties must be minimized. To achieve this, we are designing new cells fitted with high accuracy (0.1 K) temperature sensors placed along the body of the cell and inserted directly into the gas sample. The probes are suspended ~ 1 cm away from the interior cell walls to ensure that gas temperatures are measured rather than the temperature of the cell walls or the leads. In acquiring new data, we continuously monitored and were able to control the gas sample temperature to better than 0.2 K.

Knowing the exact number of molecules encountered by the optical beam requires attention to several aspects of the experiment:

- Continuous monitoring of the sample pressure during the entire period of spectral acquisition to confirm no significant change in the cell pressure;
- Accurate calibration of the capacitance manometers;
- Gas samples calibrated by mass spectrometry;
- Evacuated light paths to ensure that there are no absorption by CO_2 or other gases within the cell from any part of the light path outside of the cell;
- New stainless steel cells dedicated to CO_2 spectroscopic measurements with no detectable residuals due to contaminant species (e.g., H_2O);
- Pressures of pure CO_2 greater than 10 Torr so that outgassing from the walls is not significant;
- Correction for the partial pressure of CO_2 dimers in high pressure samples [27];
- Knowledge of the absorption path length;
- Characterization of the 0% and 100% transmission levels.

The sample pressure is measured using capacitance manometers (MKS Baratron) calibrated against NIST standards and with measurement uncertainties of 0.1% of the full-scale readout. Thus, the pressure measurement uncertainties are 1 Torr for 100 Torr $\leqslant P \leqslant$ 1000 Torr, 0.1 Torr for 10 Torr $\leqslant P \leqslant$ 100 Torr, and 0.01 Torr for 1 Torr $\leqslant P \leqslant$ 10 Torr. In practice, we found that once the cell temperature became stable, the measured sample pressures became stable to 0.1%.

The uncertainties in the optical path length and abundance of the absorbing species propagate on a one-to-one basis into the accuracies of the measured line intensities. Path lengths are varied from 0.347–121 m to obtain spectra providing a wide sampling of transition intensities, as well as estimates of the overall uncertainly. To maintain knowledge of the composition and purity of the gas samples, we employ the rigorous gas handling protocols established by the NOAA Climate Modeling and Dynamics Laboratory (CMDL) for use in calibrating the GLOBALVIEW-CO_2 network [3,28]. All gas samples are taken from rigorously calibrated, ultra-high purity gas cylinders for which the abundances of the carbon dioxide isotopologues have been determined to $\pm 0.03\%$ from mass spectral analysis. Each gas cylinder has a dedicated high-purity brass regulator passivated at high pressures prior to use. All gas transfer lines and valves are made of stainless steel. Absorption cells are constructed of stainless steel and dedicated to CO_2 spectroscopy to minimize contamination and adsorption/desorption from the cell walls. We also obtained spectra using isotopically enriched CO_2 samples (e.g., $^{13}CO_2$, $^{12}C^{18}O_2$). Special care is taken to eliminate out gassing of residual CO_2 with a natural isotopic distribution from the cell walls in such experiments.

An excellent characterization of the 0% (zero level) and 100% transmission levels is critical to the determination of intensities with sub-1% accuracies. An error of 0.1% in zero level propagates into a systematic intensity error of at least 0.1%, and this error may be even greater if the line is not entirely in the linear portion of the curve of growth. The setting of the 100% transmission level is even more important. In particular, the 100% transmission can fit out many of the non-Voigt line shape effects, especially line mixing. We ensure that the zero level is consistent where the signal is zero: in the cores of saturated lines and in regions outside of the spectral filter bandpass. If the spectrum contains saturated lines, then the zero level parameter may be floated as an additional test of the multispectrum retrieval. An accurate determination of the 100% transmission level is more difficult, even when constraining it by including empty cell spectra in the data set, but the multispectrum technique does much of this work as it forces internal consistency from spectrum to spectrum. It is also essential to extend the wavenumber range as far as possible in each spectrum to define the 100% transmission level well outside the absorption band and not to allow discontinuities in the 100% level within the absorption band. This means that we do not overfit the 100% level by using a large number of parameters, each valid over only a short wavenumber range.

2.3. Spectral calibration

The line positions of each CO_2 spectrum are calibrated by simultaneously recording the spectra of the $(2 \leftarrow 0)$ band of CO near 4200 cm^{-1} [29] and the C_2H_2 $(\nu_1 + \nu_3)$ combination band near 6500 cm^{-1} [30–32]. The line positions in each band have been measured to extremely high accuracy using frequency heterodyning. This calibration procedure yields CO_2 line position measurements accurate to $\pm 2 \times 10^{-5}$ cm^{-1}. This accuracy is comparable to that achieved in the analysis of CO_2 spectra recorded in mid-infrared (600 to 3000 cm^{-1}). Separate cells are used for CO_2 and the CO plus C_2H_2 calibration mixture; both cells are placed in the FTS optical beam and scanned simultaneously with each CO_2 spectrum.

3. Improving the multispectrum retrieval algorithm

The William and Mary multispectrum fitting algorithm was implemented more than a decade ago as a FORTRAN program running on Windows-based computers [33]. Through the years it has evolved to deal with spectra recorded using a variety of instruments such as different types of Fourier transform spectrometers, tunable diode laser spectrometers as well as various molecular species. The code now includes flexible modeling of spectrometer-induced distortions. For Fourier transform spectra the residual phase error, effective apodization, zero transmission and continuum levels may be fitted to each experimental spectrum. For example, it was used to retrieve individual line parameters of the CO_2 laser bands at 10 μm [15,16] by measuring simultaneously about 30 pure and foreign-gas broadened spectra. In Table 2, an evaluation of possible error sources from that study is given, and the combined effects were estimated to be around 2%. Nevertheless, the integrated intensities of the two laser bands were found to be within 1.2 and 0.2% of values reported by Dana et al. [34]; at the time, this work represented the state-of-the-art for simple molecules using spectra recorded at high resolution (0.006 cm^{-1}) and modest signal to noise ratios $(300 : 1)$.

A crucial test of the calibration accuracy is whether we can fit the best calibrated spectra without systematic residuals and without empirical adjustment to any experimental state parameters. The multispectrum technique can derive line/band intensities to 'statistical precisions' better than 0.1%. The systematic uncertainties, especially errors in the experimental state parameters, overwhelm the internal uncertainties. The multispectrum technique can determine spectrum line halfwidths with an uncertainty better than 0.1%, but the systematic uncertainties have always limited the absolute accuracy of halfwidths determined from experimental spectra to 1–2%. The multispectrum technique can be used as a powerful tool for identifying and reducing the experimental uncertainties since the amount of empirical adjustment required to simulate the experimental spectra accurately is a metric of how well we are actually measuring the experimental state parameters. This information can then be used to improve the measurement of the experimental state.

Studies of CO bands provide clear evidence that the standard Voigt line shape function fails to reproduce the observed line shapes in high resolution spectra with very high signal to noise [35–39]. Fig. 3 demonstrates that speed-dependent Voigt profiles with line mixing must be used to obtain a satisfactory fit for saturated CO P- and R-branch transitions [35]. In Fig. 3, the residual differences between the theoretical calculation of intensities and the observed values from Devi et al. [40] and Zou and Varanasi [41] can be traced to use of the wrong line shape for the retrievals. We note that hints of such problems appeared in past CO_2 studies (see Fig. 4 from Devi et al. [15]). The dilemma was that line mixing was masked in the retrieval process because the least squares algorithms adjusted the individual positions, intensities and widths to compensate for the discrepancies actually

Table 2
Retrieval error sources from the multispectral fits of Devi et al. [15,16]

Error source	Uncertainty
Pressure (calibration)	< 1.0%
Temperature	0.2%
Zero level	0.3%
Continuum level	0.1%
Phase error	0.1%
Path length	0.1%
Composition	< 0.05%
Channel spectrum correction	0.01%
Sample purity	< 0.01%
Instrument (ILS) and molecular line shape	Not quantified
RMS total	2.0%

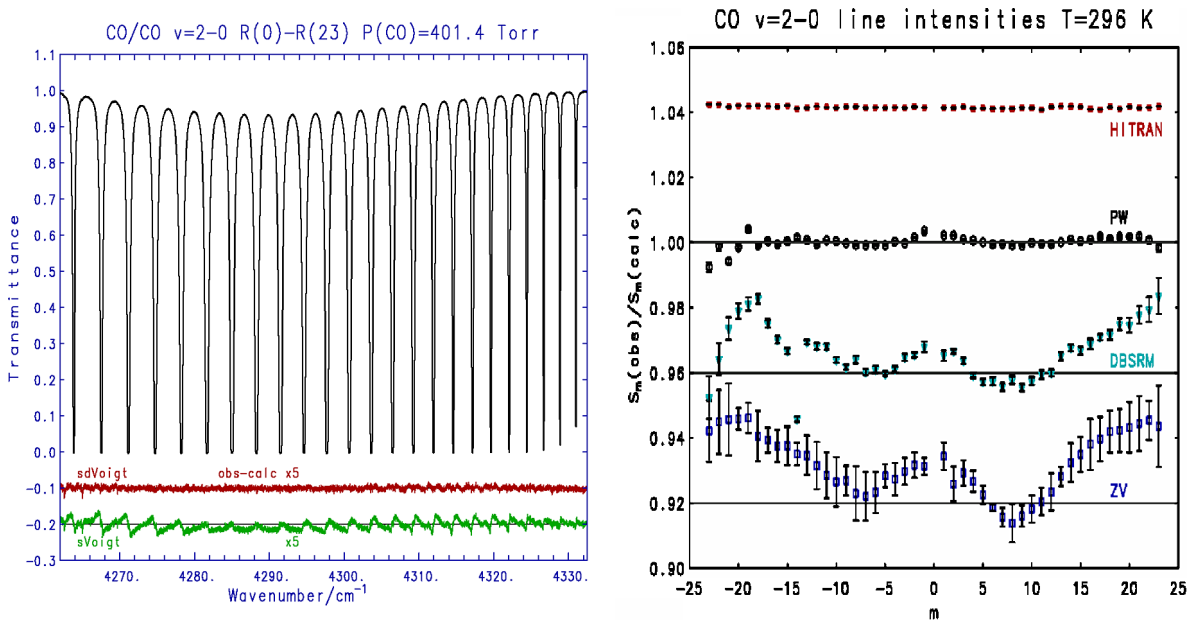

Fig. 3. The importance of molecular line shape in retrieving line intensities. Left: A pure CO spectrum recorded with the Kitt Peak FTS at 0.011 cm^{-1} resolution [35]. The transitions are modeled using a speed-dependent Voigt line shape with line mixing. Without line mixing, there are systematic residual differences. Right: The bottom three traces show the ratio of measured line intensities to corresponding values calculated by quantum mechanical models for three studies: PW [35]; DBSRM [40] and ZV [41] used standard Voigt profiles. The ratios are offset for clarity; the horizontal lines represent a ratio = 1.0. The top trace compares two theoretical calculations (HITRAN 2000/PW).

caused by incorrect molecular line shapes. This apparently occurred even in the Brault et al. study (PW in Fig. 3 [35]); the observed intensities were adjusted individually and therefore do not completely agree with calculated values.

To deal with this problem, we returned to the whole band retrieval technique imagined by Shaw and coworkers in the 1980s [42,43]. Rather than adjusting transition positions and intensities on a line-by-line basis, we modified the multispectrum retrieval software to iterate the values of the rovibrational constants G, B, D and H for the upper and lower state energies and the transitions moment constants (vibrational band strength S_v and Herman–Wallis-type parameters a_1, a_2, a_3 and a_4)

$$E = G_v + \left(B'J'[J'+1] - D'\left\{J'[J'+1]\right\}^2 + H'\left\{J'[J'+1]\right\}^3\right) - \left(B''J''[J''+1] - D''\left\{J''[J''+1]\right\}^2 + H''\left\{J''[J''+1]\right\}^3\right) \quad (1)$$

$$S_i = \frac{S_v \nu_i L_i F}{Q_r \nu_0} \exp\left(\frac{C_2 E''}{T_0}\right)\left[1 - \exp\left(\frac{C_2 \nu_i}{T_0}\right)\right] \quad (2)$$

$$F = \left(1 + a_1 m + a_2 m^2 + a_3 m^3 + a_4 J(J+1)\right)^2 \quad (3)$$

where the term $a_4 J(J+1)$ in Eq. (3) applies only to bands with Q-branches and is indistinguishable from the a_2 term in P- and R-branches. The individual 'measured' positions were constrained to positions calculated with Eq. (1) and the 'measured' intensities were constrained to intensities calculated with Eq. (2). As a test of the procedure, the band centered near 6345 cm^{-1} was fitted simultaneously using six spectra of pure CO_2 with pressures ranging from 11.01 to 896.84 Torr at room temperature. A typical retrieval is shown in Fig. 5. The lowest panel has the observed spectra, and the other four are the differences between observed and computed spectra. As seen here, it was immediately apparent that the constrained fit could not be made to converge to the level of the spectral signal to noise ratios using only the ordinary Voigt profile. Introduction of line mixing via the Rosenkranz formulation [44] greatly improved the standard deviation of the fit for the whole band.

Closer inspection of the individual transitions revealed that there are still some small discrepancies between the observed and synthetic spectra, even for those that included Rosenkranz line mixing. Two other line shape functions were used in an attempt to improve the results: a Voigt profile with line mixing using the relaxation matrix elements, as described by Levy et al. [45] and a speed dependent profile with line mixing calculated using the relaxation matrix elements (see [46–48]). To illustrate the sensitivities of the line parameters on line shape, the differences between the values obtained from the Speed Dependent Voigt profile with the relaxation matrix formulation of line mixing and the other three line shapes are shown in Table 3 for two transitions. The first column lists the parameter examined, and the next three columns have the differences

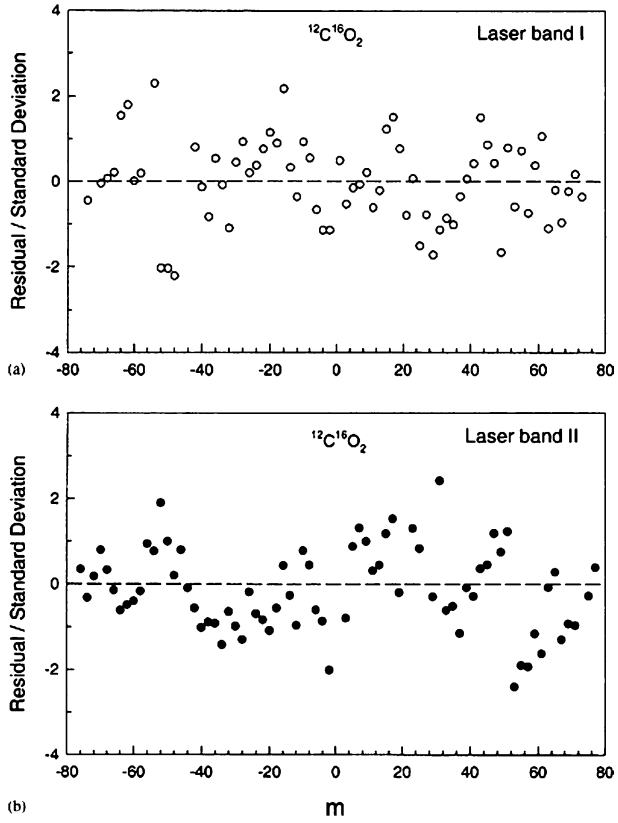

Fig. 4. Percent differences between retrieved and calculated line intensities for 10 μm CO_2 bands [15]. The inadequacy of the Voigt line shape produced systematic residuals in the simulated intensities, despite the fact that the RMS uncertainties suggested that the observed spectra were reproduced to within the experimental signal to noise ratio of 300 : 1.

Table 3
Differences in $^{12}CO_2$ line parameters determined using different line shape functions

Line parameter	Differences		
	Voigt and Relaxation Matrix	Voigt and Rosenkranz	Voigt only
RMS whole band	0.0828%	0.0832%	0.0945%
$P(10)$ 6339.7086 cm^{-1}			
ν (cm^{-1})	−0.000004	−0.000001	−0.000007
Shift δ^0 (self)	−0.00001	0.00014	0.00092
Intensity	−0.68%	−0.74%	−1.05%
Width b_L^0 (self)	−0.70%	−0.64%	1.30%
$R(10)$ 6355.9388 cm^{-1}			
ν (cm^{-1})	0.000003	−0.000001	−0.000006
Shift δ^0 (self)	−0.00000	−0.00029	−0.00118
Intensity	−0.72%	−0.75%	−1.12%
Width b_L^0 (self)	−0.61%	−0.67%	1.17%

Values with other line shapes are compared to those with Speed Dependence Voigt (SDV) line shape [47], with Relaxation Matrix elements (RM) [45]. Intensity and width differences are computed as (other − SDVRM)/SDVRM × 100%.

obtained, respectively, using (a) normal Voigt with relaxation matrix, (b) normal Voigt with Rosenkranz line mixing and (c) normal Voigt without line mixing. Differences in line positions are in cm^{-1} and pressure shifts are in $cm^{-1}\,atm^{-1}$ while the values for intensity and width are in percent. The RMS values of the retrieval for the three of the fits in Fig. 5 are listed; the RMS of the Speed Dependent Voigt profile with the relaxation matrix formulation of line mixing is the smallest (0.0815%).

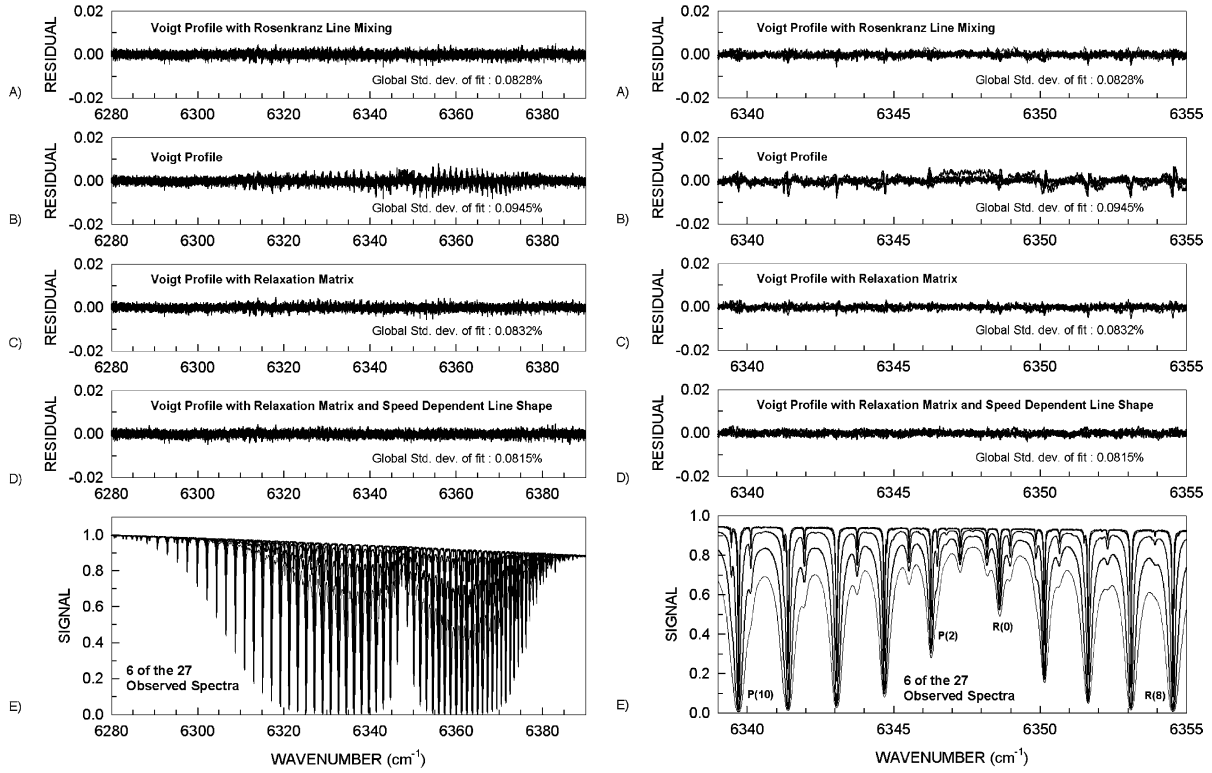

Fig. 5. Left: 6 self-broadened spectra recorded with a natural CO_2 sample recorded with the Kitt Peak FTS and a 6-m base path White cell. The path length range from 25 to 49 m and CO_2 pressures vary from 11 to 897 Torr. We used a multispectrum fitting technique to fit 27 spectra simultaneously (6280 to 6395 cm^{-1}) that included 16 self-broadened and 11 air-broadened spectra. For clarity we show only 6 self-broadened spectra in these figs. Right: we have re-plotted a short spectral interval (6339 to 6355 cm^{-1}) to illustrate the effect of different line shape functions in fitting the region near the center of the 30012 ← 00001 band. In the bottom panel (E) in both sets, we have plotted the observed spectra. In panels (A) through (D), we show the fit residuals from using (A) Voigt line shape with Rosenkranz line mixing (B) Voigt line shape (C) Voigt line shape with line mixing calculated using the relaxation matrix elements and (D) Voigt line shape with line mixing calculated using relaxation matrix elements and the speed-dependent line shape. The residuals plotted here are actually taken from a 27-spectra fit.

The results presented in Table 3 show that while the choice of line shape function only affects the RMS residual of the entire multispectrum fit at the 0.1% level, it impacts the intensities of individual transitions at the 1% level, and, therefore, must be critically evaluated for applications requiring sub-1% uncertainties such as OCO. The line intensities and line widths are both underestimated by about 0.7% when speed dependence of the line shape function is neglected; omitting line mixing increases the discrepancy to approximately -1% for each parameter. There is no impact on the retrieved line positions since the differences are all less than 1×10^{-5} cm^{-1} and within the experimental measurement uncertainty of $\pm 2 \times 10^{-5}$ cm^{-1}. The pressure shift parameters differ by a factor of 100 when line mixing is omitted and by a factor of 10 when using different expressions for the line mixing coefficients (Rosenkranz versus relaxation matrix). These results require further investigation before we can offer a quantitative explanation.

4. Conclusion

OCO X_{CO_2} remote sensing requirements place unprecedented demands on the CO_2 spectroscopic parameters, yet the preliminary results presented here demonstrate that it should be possible to determine intensities and line shape parameters to the required 0.3% accuracy. Our preliminary analysis of several near infrared CO_2 bands shows that they are well characterized using standard Voigt line shapes combined with weak line mixing despite the fact that these bands lack Q-branches and the transitions in both the P- and R-branches are spaced by ~ 1 cm^{-1}. It is possible that Dicke narrowing, line mixing and speed dependence all occur simultaneously; however, this is revealed only in a simultaneous analysis of high signal-to-noise spectra recorded over a range of pressures and for which the experimental state has been well defined. We also find that it is necessary

to constrain the line positions and intensities to reasonable values to assess line shapes accurately. A similar conclusion has recently been reached by Niro, Hartmann and coworkers in their recent studies of the CO_2 spectrum [49–52].

Our analysis required no new physics, but the results imply that remote sensing retrievals need to include state-to-state interactions explicitly to reproduce the observed radiances quantitatively. This is tractable for small linear molecules; however, implementing this approach for many non-linear molecules, for example H_2O or CH_4, is currently unfeasible since we lack accurate theoretical models to describe the rovibrational energy levels beyond the fundamental regions, In addition, the computational resources required to perform such calculations are daunting. Nevertheless, once these challenges are met, spectral analysis will no longer require a multiple-step process of retrieving individual spectroscopic parameters from different spectra and then modeling them with quantum mechanics. We thus envision a single step analysis mode in which improved accuracies for line parameters can be extracted directly from laboratory spectra. For now, we are encouraged that the targeted accuracy of 0.3% for OCO will be reached through our laboratory studies now in progress.

Acknowledgements

The authors wish to thank Claude Plymate and Mike Dulick of the National Solar Observatory for assistance in obtaining the data recorded at Kitt Peak. The research at the Jet Propulsion Laboratory (JPL), California Institute of Technology, was performed under contract with National Aeronautics and Space Administration. We also thank NASA's Upper Atmosphere Research Program for support of the McMath-Pierce FTS laboratory facility. The material from the College of William & Mary is based upon work supported by the National Science Foundation under Grant ATM-0338475.

References

[1] R.F. Keeling, S.R. Shertz, Seasonal and interannual variations in atmospheric oxygen and implications for the global carbon-cycle, Nature 358 (1992) 723–727.
[2] J.T. Houghton, Y. Ding, D.J. Griggs, M. Noguer, P.J. van der Linden, X. Dai, K. Maskell, C.A. Johnson (Eds.), Climate Change 2001: The Scientific Basis. Contribution of Working Group I to the Third Assessment Report of the Intergovernmental Panel on Climate Change, Cambridge Univ. Press, Cambridge, UK and New York, 2001, 881 pp.
[3] R.C. Schnell, D.B. King, R.M. Rosson, Climate modeling and diagnostics laboratory summary report No. 25 (1998–1999), Report No. 25, 2001 and GLOBALVIEW-CO_2: Cooperative atmospheric integration project—carbon dioxide, NOAA CMDL, Boulder, CO, http://www/cmdl/noaa/gov/ccgg/globalview/co2, 2001.
[4] P.M. Cox, R.A. Betts, C.D. Jones, S.A. Spall, I.J. Totterdell, Acceleration of global warming due to carbon-cycle feedbacks in a coupled climate model, Nature 408 (2000) 184–187.
[5] P. Friedlingstein, L. Bopp, P. Ciais, J.L. Dufresne, L. Fairhead, H. LeTreut, P. Monfray, J. Orr, Positive feedback between future climate change and the carbon cycle, Geophys. Res. Lett. 28 (2001) 1543–1546.
[6] P.J. Rayner, D.M. O'Brien, The utility of remotely sensed CO_2 concentration data in surface source inversions, Geophys. Res. Lett. 28 (2001) 175–178.
[7] D. Crisp, et al., The Orbiting Carbon Observatory (OCO) mission, Adv. Space Res. 34 (2004) 700.
[8] C.E. Miller et al., Precision requirements for space-based X_{CO_2} data, J. Geophys. Res., submitted for publication.
[9] A. Chedin, A. Hollingsworth, N.A. Scott, S. Serrar, C. Crevoisier, R. Armante, Annual and seasonal variations of atmospheric CO_2, N_2O and CO concentrations retrieved from NOAA/TOVS satellite observations, Geophys. Res. Lett. 29 (2002), doi:10.1029/2001GL014082.
[10] M.J. Christi, G.L. Stephens, Retrieving profiles of atmospheric CO_2 in clear sky and in the presence of thin cloud using spectroscopy from the near and thermal infrared: A preliminary case study, J. Geophys. Res. 109 (2004), doi:10.1029/2003JD004058, D04316.
[11] R.J. Engelen, A.S. Denning, K.R. Gurney, G.L. Stephens, Global observations of the carbon budget. 1. Expected satellite capabilities for emission spectroscopy in the EOS and NPOESS eras, J. Geophys. Res. 106 (2001) 20,055–20,068.
[12] R.J. Engelen, G.L. Stephens, Information content of infrared satellite sounding measurements with respect to CO_2, J. Appl. Meteorol. 43 (2004) 373–378.
[13] D.P. Edwards, L.L. Strow, Spectral line shape considerations for limb temperature sounders, J. Geophys. Res. 96 (1991) 20,859–20,868.
[14] M. McHugh, B. Magill, K.A. Walker, C.D. Boone, P.F. Bernath, J.M. Russell III, Comparison of atmospheric retrievals from ACE and HALOE, Geophys. Res. Lett. 32 (2005), doi:10.1029/2005GL022403, L15S10.
[15] V.M. Devi, C.D. Benner, M.A.H. Smith, L.R. Brown, M. Dulick, Absolute intensity measurements of the $^{12}C^{16}O_2$ laser bands near 10 μm, J. Quant. Spec. Rad. Transfer 76 (2003) 393–410.
[16] V.M. Devi, C.D. Benner, M.A.H. Smith, L.R. Brown, M. Dulick, Multispectrum analysis of pressure broadening and pressure shift coefficients in the $^{12}C^{16}O_2$ and $^{13}C^{16}O_2$ laser bands, J. Quant. Spec. Rad. Transfer 67 (2003) 411–434.
[17] L. Wallace, W. Livingston, Spectroscopic observation of atmospheric trace gases over Kitt Peak: 1. Carbon dioxide and methane from 1979 to 1985, J. Geophys. Res. 95 (1990) 9823–9827.
[18] Z.H. Yang, G.C. Toon, J.S. Margolis, P.O. Wennberg, Atmospheric CO_2 retrieved from ground-based near IR spectra, Geophys. Res. Lett. 29 (2002), doi:10.1029/2001GL014537.

[19] J.H. Park, Atmospheric CO_2 monitoring from space, Appl. Opt. 36 (1997) 2701–2712.
[20] C. Corsi, F. D'Amato, M. De Rosa, G. Modugno, High-resolution measurements of line intensity, broadening and shift of CO_2 around 2 μm, Eur. Phys. J. D 6 (1999) 327–332.
[21] M. de Rosa, C. Corsi, M. Gabrysch, F. D'Amato, Collisional broadening and shift of lines in the $(2\nu_1 + 2\nu_2 + \nu_3)$ band of CO_2, J. Quant. Spec. Rad. Transfer 61 (1999) 97–104.
[22] J. Henningsen, H. Simonsen, The $(22^01–00^00)$ band of CO_2 at 6348 cm^{-1}: linestrengths, broadening parameters, and pressure shifts, J. Mol. Spectrosc. 203 (2000) 16–27.
[23] L.S. Rothman, D. Jacquemart, A. Barbe, D.C. Benner, M. Birk, L.R. Brown, M.R. Carleer, C. Chackerian Jr., K. Chance, V. Dana, V.M. Devi, J.M. Flaud, R.R. Gamache, A. Goldman, J.-M. Hartmann, K.W. Jucks, A.G. Maki, J.Y. Mandin, S. Massie, J. Orphal, A. Perrin, C.P. Rinsland, M.A.H. Smith, R.A. Toth, J. Vander Auwera, P. Varanasi, G. Wagner, The HITRAN 2004 molecular spectroscopic database, J. Quant. Spec. Rad. Transfer 96 (2005) 139–204.
[24] M. Birk, D. Hausamann, G. Wagner, J.W. Johns, Determination of line strengths by Fourier-transform spectroscopy, Appl. Opt. 35 (1996) 2971–2985.
[25] L.P. Giver, L.R. Brown, C. Chackerian, R.S. Freedman, The rovibrational intensities of five absorption bands of $^{12}C^{16}O_2$ between 5218 and 5349 cm^{-1}, J. Quant. Spec. Rad. Transfer 67 (2003) 417–436.
[26] L.P. Giver, C. Chackerian, M.N. Spencer, L.R. Brown, R.B. Wattson, The rovibrational intensities of the $40^01 \leftarrow 00^00$ pentad absorption bands of $^{12}C^{16}O_2$ between 7284 and 7921 cm^{-1}, J. Mol. Spectrosc. 175 (1996) 104–111.
[27] Y.I. Baranov, W.J. Lafferty, G.T. Fraser, A.A. Vigasin, On the origin of the band structure observed in the collision-induced absorption bands of CO_2, J. Mol. Spectrosc. 218 (2003) 260–261.
[28] P.P. Tans, Personal communication, 2002.
[29] C.R. Pollock, F.R. Petersen, D.A. Jennings, J.S. Wells, A.G. Maki, Absolute frequency measurements of the 2–0 band of CO at 2.3 μm: calibration standard frequencies from high resolution color center laser spectroscopy, J. Mol. Spectrosc. 99 (1983) 357–368.
[30] K. Nakagawa, M. deLabachelerie, Y. Awaji, M. Kourogi, Accurate optical frequency atlas of the 1.5-μm bands of acetylene, J. Opt. Soc. Am. B—Opt. Phys. 13 (1996) 2708–2714.
[31] M. Kusaba, J. Henningsen, The $\nu_1 + \nu_3$ and the $\nu_1 + \nu_2 + \nu_4^1 + \nu_5^{-1}$ combination bands of $^{13}C_2H_2$. Linestrengths, broadening parameters, and pressure shifts, J. Mol. Spectrosc. 209 (2001) 216–227.
[32] A. Onae, K. Okumura, J. Yoda, K. Nakagawa, A. Yamaguchi, M. Kourogi, K. Imai, B. Widiyatomoko, Toward an accurate frequency standard at 1.5 μm based on the acetylene overtone band transition, IEEE Trans. Instrum. Meas. 48 (1999) 563–566.
[33] D.C. Benner, C.P. Rinsland, V.M. Devi, M.A.H. Smith, D. Atkins, A multispectrum nonlinear least-squares fitting technique, J. Quant. Spec. Rad. Transfer 53 (1995) 705–721.
[34] V. Dana, J.-Y. Mandin, G. Guelachvili, Q. Kou, M. Morillon-Chapey, R.B. Wattson, L.S. Rothman, Intensities and self-broadening coefficients of $^{12}C^{16}O_2$ lines in the laser band region, J. Mol. Spectrosc. 152 (1992) 328–341.
[35] J.W. Brault, L.R. Brown, C. Chackerian, R.S. Freedman, A. Predoi-Cross, A.S. Pine, Self-broadened $^{12}C^{16}O$ line shapes in the $v = 2 \leftarrow 0$ band, J. Mol. Spectrosc. 222 (2003) 220–239.
[36] N. Picqué, G. Guelachvili, V. Dana, J.Y. Mandin, Absolute line intensities, vibrational transition moment, and self-broadening coefficients for the 3–0 band of $^{12}C^{16}O$, J. Mol. Struct. 517 (2000) 427–434.
[37] D. Jacquermart, J.Y. Mandin, V. Dana, N. Picqué, G. Guelachvili, A multispectrum fitting procedure to deduce molecular line parameters: application to the 3–0 band of $^{12}C^{16}O$, Eur. Phys. J. D 14 (2001) 55–69.
[38] J. Henningsen, H. Simonsen, T. Mogelberg, E. Trudso, The $0 \rightarrow 3$ overtone band of CO: precise linestrengths and broadening parameters, J. Mol. Spectrosc. 193 (1999) 354–362.
[39] C. Chackerian, R.S. Freedman, L.P. Giver, L.R. Brown, Absolute rovibrational intensities and self-broadening and self-shift coefficients for the $V = 3 \leftarrow V = 0$ band of $^{12}C^{16}O$, J. Mol. Spectrosc. 210 (2001) 119–126.
[40] M. Devi, D.C. Benner, M.A.H. Smith, C.P. Rinsland, A.W. Mantz, Determination of self- and H_2-broadening and shift coefficients in the 2–0 band of $^{12}C^{16}O$ using a multispectrum fitting procedure, J. Quant. Spec. Rad. Transfer 75 (2002) 455–471.
[41] Q. Zou, P. Varanasi, New laboratory data on the spectral line parameters in the 1–0 and 2–0 bands of $^{12}C^{16}O$ relevant to atmospheric remote sensing, J. Quant. Spec. Rad. Transfer 75 (2002) 63–92.
[42] R.L. Hawkins, M.L. Hoke, J.H. Shaw, Band parameters of N_2O and CO_2 determined by whole band analysis, Proc. Soc. Photo-Opt. Instr. Eng. 289 (1981) 99–201.
[43] C.L. Lin, J.H. Shaw, Line parameters determined by spectral curve fitting, J. Opt. Soc. Am. 67 (1977) 1442.
[44] P.W. Rosenkranz, Shape of the 5 mm oxygen band in the atmosphere, IEEE Trans. Ant. Prop. AP-23 (1975) 498–506.
[45] A. Levy, N. Lacome, C. Chackerian Jr., Collisional line mixing, in: K.N. Rao, A. Weber (Eds.), Spectroscopy of the Earth's Atmosphere and Interstellar Medium, Academic Press, Boston, MA, 1992, pp. 261–337 (Chapter 2).
[46] R. Ciurylo, J. Szudy, Speed-dependent pressure broadening and shift in the soft collision approximation, J. Quant. Spec. Rad. Transfer 57 (1997) 411–423.
[47] R. Ciurylo, A.S. Pine, Speed-dependent line mixing profiles, J. Quant. Spec. Rad. Transfer 67 (2000) 375–393.
[48] R. Ciurylo, A.S. Pine, J. Szudy, A generalized speed-dependent line profile combining soft and hard partially correlated Dicke-narrowing collisions, J. Quant. Spec. Rad. Transfer 68 (2001) 257–271.
[49] F. Niro, C. Boulet, J.-M. Hartmann, Spectra calculations in central and wing regions of CO_2 IR bands between 10 and 20 μm. I: Model and laboratory measurements, J. Quant. Spec. Rad. Transfer 88 (2004) 483–498.
[50] F. Niro, F. Hase, C. CamyPeyret, S. Payan, J.-M. Hartmann, Spectra calculations in central and wing regions of CO_2 IR bands between 10 and 20 μm. II: Atmospheric solar occultation spectra, J. Quant. Spec. Rad. Transfer 90 (2005) 43–59.

[51] F. Niro, T. von Clarman, K. Jucks, J.-M. Hartmann, Spectra calculations in central and wing regions of CO_2 IR bands between 10 and 20 μm. III: Atmospheric emission spectra, J. Quant. Spec. Rad. Transfer 90 (2005) 61–76.
[52] F. Niro, K. Jucks, J.-M. Hartmann, Spectra calculations in central and wing regions of CO_2 IR bands. IV: Software and database for the computation of atmospheric spectra, J. Quant. Spec. Rad. Transfer 95 (2005) 469–481.